

## Proton Affinities of Primary Alkanols: An Appraisal of the Kinetic Method

John L. Holmes,\* Christiane Aubry, and Paul M. Mayer

Department of Chemistry, University of Ottawa, 10 Marie-Curie, Ottawa, Ontario K1N 6N5, Canada

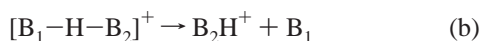
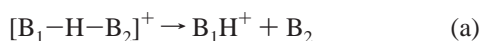
Received: October 20, 1998; In Final Form: December 17, 1998

The kinetic method is a now well-established technique for determining thermochemical properties such as acidities and proton affinities. We present here a study of the application of the kinetic method to the proton affinities (PA) of a series of homologous primary alkanols, namely ethanol through *n*-octanol. Both metastable and collisionally activated dissociations of proton-bound alkanol pairs were studied, the latter as a function of the target gas and its pressure. Plots of  $\ln([R_1OH_2^+]/[R_2OH_2^+])$  vs PA for both experiments were obtained to determine new PA values and investigate the significance of the “effective temperature” term. When the experiments are considered in detail, it is apparent that the kinetic method is essentially a semiempirical relationship, without a sound physicochemical basis.

### Introduction

The kinetic method introduced by Cooks<sup>1</sup> has provided an alternative to equilibrium measurements<sup>2</sup> and reaction bracketing experiments<sup>3</sup> for measuring thermochemical properties. This method has been widely used for the determination of gas-phase acidities, basicities, and proton affinities of organic compounds as well as the determination of affinities for ions other than the proton.<sup>1c</sup>

For proton affinities (PA) to be evaluated, proton-bound dimers,  $[B_1-H-B_2]^+$ , are generated and isolated in a mass spectrometer, and the competitive reactions (a) and (b) yielding the individual protonated monomers are investigated.



Upon fragmentation, the monomer having the greater proton affinity will preferentially carry the proton. The reactions are observed as metastable dissociations or induced by collisional excitation.

Canonical transition state theory<sup>4</sup> (which applies to species at an equilibrium thermodynamic temperature) has been applied to these systems.<sup>1</sup> The rate constant for a reaction of such a species is given by the statistical thermodynamics version of the Arrhenius equation:

$$\ln k = \ln\left(\frac{Q^\ddagger}{Q}\right) + \frac{E^\circ}{RT} \quad (1)$$

where  $Q$  and  $Q^\ddagger$  are the partition functions for the reactant and the transition state, respectively,  $E^\circ$  is the activation energy,  $R$  is the ideal gas constant, and  $T$  is the temperature. When there are two competing dissociations, their respective rate constants,  $k_1$  and  $k_2$ , are given by

$$\ln\left(\frac{k_1}{k_2}\right) = \ln\left(\frac{Q_1^\ddagger}{Q_2^\ddagger}\right) + \frac{E_2^\circ - E_1^\circ}{RT} \quad (2)$$

In the kinetic method,  $k_1$  and  $k_2$  are replaced by the respective product ion intensities  $[B_1H^+]$  and  $[B_2H^+]$ , and eq 2 is simplified to permit the evaluation of the difference in proton affinities,  $E_2^\circ - E_1^\circ = PA_2 - PA_1$ :

$$\ln\frac{[B_1H^+]}{[B_2H^+]} = (PA_2 - PA_1)\frac{1}{RT_{\text{eff}}} = \frac{\Delta PA}{RT_{\text{eff}}} \quad (3)$$

For eq 3 to apply, several assumptions are made. The most important is that the proton-bound molecular pairs have internal energy distributions that can be described by an “effective temperature” term,  $T_{\text{eff}}$ . Note that, in general, a system of isolated ions generated in a mass spectrometer cannot be assumed to have a Boltzmann distribution of internal energies, except where special efforts are made to generate thermal equilibria, such as in high-pressure mass spectrometry.<sup>5</sup>

Also, the logarithm term should represent the ratio of the fractions of ions fragmenting that have internal energies from  $E_1^\circ \rightarrow \infty$  and from  $E_2^\circ \rightarrow \infty$ , respectively. This presents a problem when studying the dissociation of metastable ions in a sector mass spectrometer, a point which will be discussed in detail later. The third assumption is that neither dissociation involves a reverse energy barrier. This is a priori likely when only simple bond cleavages are involved. Finally, it is assumed that there are no entropic effects, i.e.,  $Q_1^\ddagger = Q_2^\ddagger$ .

To use the simplified eq 3 to obtain an absolute proton affinity value, a reference base of known PA is required.

For a series of molecules having a common functionality, it has been found that a plot of  $\ln([B_1H^+]/[B_2H^+])$  vs  $\Delta PA$  yields a straight line. Thus, from the slope of the plot, a temperature-like term,  $T_{\text{eff}}$ , can be obtained. It is a common belief that this parameter relates to the average internal energy of the ion population.<sup>1</sup> If the ion population is not in thermal equilibrium with its surroundings, such as in an ion beam experiment or in partial thermal equilibrium, as in the case of high-pressure

\* Corresponding author. e-mail: jholmes@science.uottawa.ca.

experiments, the physical interpretation of the parameter obtained from the slope of the plot can be neither straightforward nor certain. A recent report by McMahon et al.<sup>6</sup> describes a study of alkyl nitrile PA values by high-pressure mass spectrometry (equilibrium measurements,  $\Delta G$  values) and the above kinetic method in which *inter alia* the “effective temperature” question was directly addressed. It was concluded that in these experiments the ion source temperature may be related to the “effective temperature”, but the inverse dependence observed could not readily be explained. In the interim, we have found evidence that the nitrile adduct ions in McMahon’s work were not metastable but were dissociating as a result of collisional excitation.<sup>7</sup>

Surprisingly few small heteroatom-containing homologous molecular series other than some amines have been investigated by this method for evaluating proton affinities.<sup>1b,c</sup> The present work was undertaken to discover whether the kinetic method is appropriate for the dissociation of proton-bound alkanols,  $(R_1OH)H^+(R_2OH)$  (for which some reliable PA values exist), to compare the method for metastable and collisionally activated ions, and to explore the significance of the “effective temperature”.

### Experimental Procedures

The proton-bound dimers were generated under CI conditions in the ion source of our modified triple-focusing (BEE) VG ZAB-2F mass spectrometer<sup>8</sup> by self-protonation of the monomers. The metastable and collision-induced dissociations<sup>9</sup> (MI and CID, respectively) of the mass-selected proton-bound dimers were studied in the second and third field-free regions of the instrument. Peak heights from individual scans were used to measure the relative abundances of the fragment ions. The ion source pressure was measured externally using an ion gauge. The ion source temperature was normally maintained at  $423 \pm 5$  K, and the inlet system was kept at a similar temperature.

The compounds were purchased from Aldrich Chemical Co. (Milwaukee, WI) and used without further purification.

### Results and Discussion

**Dissociation Characteristics of Metastable Ions.** Preliminary experiments with a wide range of primary, secondary, and tertiary alkanols showed that for the latter two classes of compounds the metastable ion (MI) mass spectra for  $(R_1OH)H^+(R_2OH)$  were often dominated by processes other than the dissociation to  $R_1OH_2^+$  and  $R_2OH_2^+$  (mainly olefin eliminations). The primary alkanols are not so disposed, and the competing reactions (a) and (b) provided the major signals in the MI mass spectra. However, the MI mass spectra of the higher homologues also showed a weak (<10%) water loss signal and small signals corresponding to olefin eliminations (abundances were  $3 \pm 2\%$ , except for isobutanol, where it is  $\sim 12\%$ ). These minor peaks were insensitive to the presence of collision gas whereas reactions (a) and (b) were affected.

For the higher homologues,  $R = n-C_5H_{11}OH$  to  $n-C_8H_{17}OH$ , the MI spectra of the adduct ions also showed the consecutive loss of  $H_2O$  from the  $ROH_2^+$  product. On transmitting these metastably generated  $ROH_2^+$  ions to the third field-free region, it was observed that they were themselves metastable with regard to  $H_2O$  loss. For these homologues, when calculating  $\ln([R_1OH_2^+]/[R_2OH_2^+])$ , the sum of the abundances  $[R_1OH_2^+ + R_1^+]$  and  $[R_2OH_2^+ + R_2^+]$  were used. As will be discussed in a future publication, this secondary reaction provides a comparative measure of the internal energy of a given  $R_1OH_2^+$  ion prepared from different  $(R_1OH)H^+(R_2OH)$  adducts.

**TABLE 1: Product Ion Ratios (*R*) for Metastable Dissociations of Proton-Bound Alkanol Pairs**

alkanol pair $R_1OH, R_2OH$	<i>R</i> $[R_2OH_2^+]/[R_1OH_2^+]$	$\ln(R)^a$
<i>n</i> -C <sub>2</sub> H <sub>5</sub> OH, <i>n</i> -C <sub>3</sub> H <sub>7</sub> OH	$37 \pm 2$	3.6 (1.16)
<i>n</i> -C <sub>3</sub> H <sub>7</sub> OH, <i>n</i> -C <sub>4</sub> H <sub>9</sub> OH	$8.6 \pm 2$	2.15
<i>n</i> -C <sub>2</sub> H <sub>5</sub> OH, <i>i</i> -C <sub>4</sub> H <sub>9</sub> OH	$410 \pm 20$	6.0
<i>n</i> -C <sub>2</sub> H <sub>5</sub> OH, <i>n</i> -C <sub>4</sub> H <sub>9</sub> OH	$295 \pm 15$	5.7 (2.06)
<i>n</i> -C <sub>3</sub> H <sub>7</sub> OH, <i>i</i> -C <sub>4</sub> H <sub>9</sub> OH	$11 \pm 1$	2.4 (0.75)
<i>n</i> -C <sub>3</sub> H <sub>7</sub> OH, <i>n</i> -C <sub>5</sub> H <sub>11</sub> OH	$25 \pm 1$	3.2
<i>n</i> -C <sub>4</sub> H <sub>9</sub> OH to <i>n</i> -C <sub>5</sub> H <sub>11</sub> OH	$3.0 \pm 0.2$	1.1 (0.59)
<i>n</i> -C <sub>5</sub> H <sub>11</sub> OH, <i>n</i> -C <sub>6</sub> H <sub>13</sub> OH	$2.0 \pm 0.1$	0.70 (0.18)
<i>n</i> -C <sub>5</sub> H <sub>11</sub> OH, <i>n</i> -C <sub>7</sub> H <sub>15</sub> OH	$3.8 \pm 0.2$	1.33
<i>n</i> -C <sub>5</sub> H <sub>11</sub> OH, <i>n</i> -C <sub>8</sub> H <sub>17</sub> OH	$5.2 \pm 0.3$	1.65

<sup>a</sup> Values in parentheses are for CID processes.

Two other observations must now be discussed. The fraction of adduct ion flux that dissociated in the field-free regions was dependent on the measured ion source pressure, but the  $\ln([R_1OH_2^+]/[R_2OH_2^+])$  ratio was essentially independent thereon. For example, the flux of the  $(C_2H_5OH)H^+(n-C_3H_7OH)$  adduct ions increased by a factor of ca. 800 over the ion source pressure range  $10^{-5}$  to  $10^{-4}$  mbar, and the degree of dissociation dropped from 18% at the lower pressure to 2.5% at the higher pressure. Thus, a greater proportion of the cluster ions are being “cooled” at higher ion source pressures (i.e., their internal energy distribution is shifted toward lower internal energy). However, the  $[n-C_3H_7OH_2^+]/[C_2H_5OH_2^+]$  ratio remained in the range  $37 \pm 2$ . This ratio was also unchanged within the same experimental reproducibility by altering the ion source temperature from 330 to 570 K.

It is apparent, therefore, that the internal energy distribution of the adduct ions, which was clearly dependent on ion source pressure, has little or no effect on the metastable ion observations reported here. This is in keeping with the nature of the MI experiment itself, which is discussed below.

**Metastable Ion Experiments.** The product ion ratios for metastable dissociations of the proton-bound pairs measured in this study are shown in Table 1. The MI experiments described in this paper do not fulfill the two main criteria for the application of the absolute rate theory expressions. The adduct ions are not completely equilibrated to the ion source temperature,  $\sim 420$  K. We know this because at this temperature, the fraction of adduct ions that would be metastable is negligibly small.<sup>10</sup> In addition, this experiment observes the dissociation of ions through a *narrow* time window (and hence internal energy window and not from  $E^\circ \rightarrow \infty$ ). For 8 kV ions of  $m/z$  185 (about the average mass of the adduct ions studied here) the time to traverse the third field-free region is ca. 12  $\mu s$ , the entering ions being approximately 29  $\mu s$  old. Figure 1 shows the fraction of the ions dissociating,  $dn/n_0$ , by a first-order process in this time frame as a function of the rate constants, which lie between ca.  $1 \times 10^2$  and  $2 \times 10^5$  s<sup>-1</sup>. Also shown on the right of Figure 1 are two representative  $\log k$  vs internal energy ( $E$ ) curves. The displacement between them ( $E_2^\circ - E_1^\circ$ ) represents the difference in proton affinities of two alkanols. The internal energy range corresponding to observations in the metastable time frame is shown as  $dE$ . Note that the energy ranges shown here do not overlap. This is a necessary condition if, as was common among the present results, the peak height ratios are ca. 10 or greater. Note also that for the more energy-demanding path, reaction b, metastable ions for this route have internal energies that correspond to much faster dissociations for reaction a, i.e., not appropriate for the metastable time frame.

The  $\ln([R_1OH_2^+]/[R_2OH_2^+])$  vs PA plot for the C<sub>2</sub> to C<sub>8</sub> alkanols is shown in Figure 2. In view of the shortcomings of

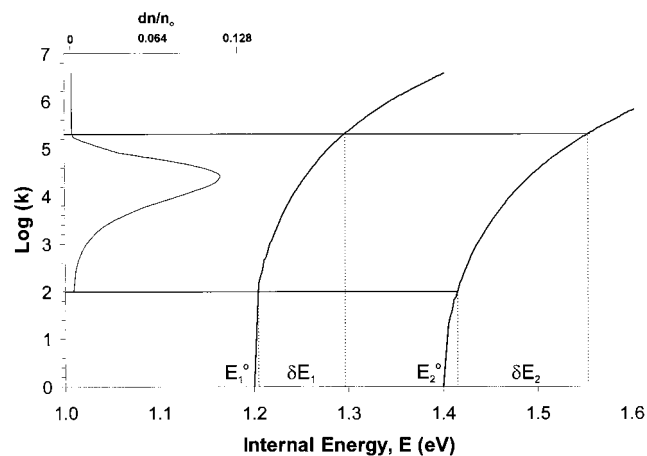


**Figure 1.** A plot of the  $\log k$  vs internal energy ( $E$ ) curves for two simple bond cleavage reactions. The curves were generated using the standard RRKM expression,<sup>4</sup> the sums and densities of states obtained via the direct count algorithm. The model compound used to generate the curves was the proton-bound methanol dimer, and the vibrational frequencies were from ab initio calculations.<sup>13</sup> Superimposed on the left side of the graph is a plot of the distribution of rate constants that contribute to metastable ion dissociations in the third field-free region of our instrument. The energy windows for metastable dissociations are shown by  $dE_1$  and  $dE_2$ .

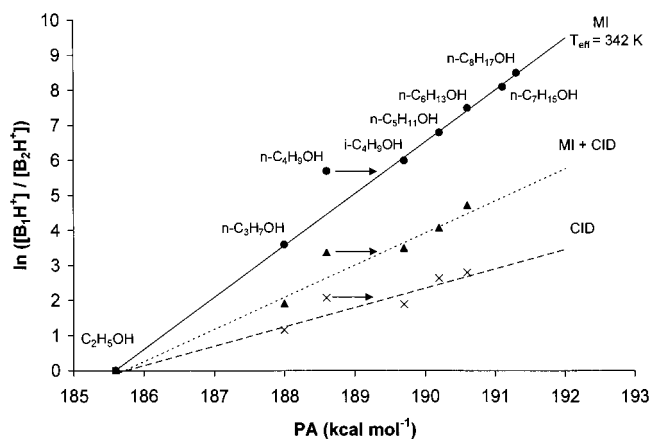


**Figure 2.** Plot of  $\ln([R_1OH_2^+]/[R_2OH_2^+])$  vs PA, as obtained from MI mass spectra (●), for eight primary alcohols ranging from ethanol through to *n*-octanol. The values were derived using the raw data in Table 1 for the various proton-bound alkanol pairs. Plots of the ratio from mixed MI and CID mass spectra (MI + CID, ▲) and isolated CID mass spectra (×) are also shown.

these MI experiments with respect to theory, it is remarkable that a straight line is obtained. However, the “effective temperature”, 342 K, derived from the slope is unlikely to have any physicochemical significance since it was not possible, by changing experimental parameters, to significantly alter the ratio of adduct ion fragmentations, but only the fraction of the total number of metastable adduct ions that could fragment. Thus, the ratio of the fragment ion abundances is independent of the adduct ion internal energy distribution in these experiments.

This point is illustrated by the following example. As shown in Figure 1, metastable ions are only observed in narrow energy segments. If the distribution of internal energies of the adduct ions can be represented as a simple exponential function, the relative areas above each energy segment will be equal to  $[B_1H^+]/[B_2H^+]$ , i.e., the ratio of the products from the competing dissociation pathways. Under these conditions, the relative areas remain unchanged by moving such a distribution up or down the internal energy scale (keeping  $E_2^\circ - E_1^\circ$  constant); only

their absolute magnitudes change. Thus, for higher internal energies a greater fraction of the total flux of adduct ions dissociates. This is in keeping with the experimental observations described above.

As mentioned above, the adduct ion internal energies and their range, which contribute to the two competing metastable ion dissociations, are themselves different (Figure 1). Klots<sup>4</sup> has derived relationships for the fragmentation of internal-energy-selected cluster ions that treat the ions as if they were at a particular temperature. This temperature is related to the average internal energy of the dissociating ion. Using these expressions, Klots has been able to calculate canonical properties of dissociating ions such as entropies of activation and heat capacities, even though the dissociating ensemble is strictly non-Boltzmann. In this sense, the metastable ions undergoing the competing dissociation reactions (which are effectively internal-energy-selected ions) have two different “temperatures”, a single temperature-like term being unsuitable for describing both metastable channels simultaneously. Nor is it apparent that the dissociations of homologous metastable cluster ions should be related to a common temperature (as predicted by eq 3). The binding energy of the higher homologues in Figure 2 is essentially constant with dimer size, ca. 30 kcal mol<sup>-1</sup>. The kinetic shift (and hence the internal energy) of the clusters will increase significantly with increasing size (due to an increase in the density-of-states of the cluster ion), and thus the “temperature” of the dissociating clusters must also effectively increase with size. Also, to a minor extent, the metastable ion window itself shifts for ions of increasing mass, larger ions having lower translational velocities. With these points in mind, relating the slope of  $\ln([B_1H^+]/[B_2H^+])$  vs PA lines to a single thermodynamic temperature is clearly unsound.

**Collision-Induced Dissociation Experiments.** In addition to MI mass spectra, collision-induced dissociation (CID) experiments are also performed on sector mass spectrometers to obtain PA values by the kinetic method (Table 1). Note that the product ion ratios from such experiments are always smaller than those from MI results alone (Figure 2). This is compatible with a much greater internal energy range being observed for these dissociating ions, corresponding now to the relative adduct ion populations from  $E_1^\circ$  and  $E_2^\circ$  to, effectively,  $\infty$ , the time scale of the observations now commencing at the moment of collisional excitation, ca.  $10^{-12}$  s. Thus, unlike MI experiments, CID experiments satisfy the second major criterion governing the application of eq 3. The kinetic energy release values for collision-induced dissociations of the  $(R_1OH)H^+(R_2OH)$  ions were typically 10–15% larger than for the corresponding metastable ion fragmentations, in keeping with the wider energy window available to the former.

In general, proton-bound molecular pairs do not show an excessive amount of other dissociations upon collisional activation, being still dominated by reactions (a) and (b). Commonly, to determine  $\ln([B_1H^+]/[B_2H^+])$  ratios from these experiments, the mixed MI and CID peak heights are used. In a CID experiment using a sector mass spectrometer, there are three time frames to consider: from entry of the field-free region to the collision cell (MI processes only), inside the collision cell (CID processes plus a minor MI contribution), and from the cell to the next analyzer (MI processes and collisionally excited ions having sufficient energy to dissociate in this region). Unless steps are taken otherwise, the peaks recorded in these “CID” mass spectra result from a combination of all three processes. The practice of using these mixed MI and CID mass spectra to generate  $\ln([B_1H^+]/[B_2H^+])$  data does not have a scientific basis

**TABLE 2: Effect of Target Gas on the Ratio  $[R_1OH_2^+]/[R_2OH_2^+]$  from CID Mass Spectra<sup>a</sup>**

experiment	target gas (pressure, mbar $\times 10^8$ )			
	He (4)	He (20) <sup>b</sup>	Ar (15)	Ar (60) <sup>b</sup>
	$(C_2H_5OH)H^+(n-C_3H_7OH)$			
CID + MI	5.8 (1.8)	3.5 (1.3)		4.5 (1.5)
CID	3.3 (1.2)	3.3 (1.2)		3.2 (1.2)
residual MI	18 (2.9)	14 (2.6)		15 (2.7)
MI = 37				
	$(n-C_5H_{11}OH)H^+(n-C_6H_{13}OH)$			
CID + MI	2.0 (0.69)	1.6 (0.47)	1.9 (0.64)	1.6 (0.47)
CID	1.3 (0.26)	1.2 (0.18)	1.2 (0.18)	1.2 (0.18)
residual MI	2.1 (0.74)	1.9 (0.64)	2.1 (0.74)	1.9 (0.64)
MI = 2.7				

<sup>a</sup> Values for  $\ln([R_1OH_2^+]/[R_2OH_2^+])$  are shown in parentheses.

<sup>b</sup> Pressures for 10% adduct ion beam reduction.

and leads to a poorer straight line (Figure 2). In addition, the mixed MI and CID mass spectra will change not only with the pressure of collision gas in the cell but also on the nature of the gas, since different gases have different collision cross sections.

The practice of applying a potential to the collision cell to separate MI and CID processes is very useful. Dissociations in the collision cell now produce fragment ion peaks displaced from their normal position<sup>15</sup> and will contain a minimal contribution from MI products, provided that the length of the cell is much less than that of the field-free region which contains it (typically <5% in our apparatus). These displaced CID mass spectra, corrected for the minor MI contribution (isolated CID mass spectra), yield a  $\ln([B_1H^+]/[B_2H^+])$  vs PA plot that is also less well described by a straight line (Figure 2). Note that the nondisplaced peaks will be a mixture of the MI mass spectrum plus the late dissociating collisionally excited ions.

These points are well illustrated by the results for the  $(C_2H_5OH)H^+(n-C_3H_7OH)$  and  $(n-C_5H_{11}OH)H^+(n-C_6H_{13}OH)$  adduct ions shown in Table 2. Clearly, the product ion ratio for the isolated CID data is *independent* of the target gas whereas the mixed MI and CID results show an apparent collision gas dependence even where the same adduct ion beam flux reduction was used. Using the isolated CID mass spectra, it is apparent that the two target gases do not produce significantly different energy distributions within the activated adduct ions. They apparently do so in the mixed MI and CID mass spectra. It is clearly essential, therefore, to separate these phenomena before applying physicochemical arguments to the results. In terms of  $\ln$  plots, the smaller  $[R_1OH_2^+]/[R_2OH_2^+]$  ratios from CID mass spectra will produce plots for  $\ln([R_1OH_2^+]/[R_2OH_2^+])$  vs PA values of lower slope than those for MI data (Figure 2). Note that the  $\ln$  function becomes hypersensitive toward the peak height ratio when it is close to 1, resulting in  $\ln$  values that are apparently quite distinct, as is the case for  $(n-C_5H_{11}OH)H^+(n-C_6H_{13}OH)$  (Table 1). Clearly here, the different  $\ln$  values derived from the isolated CID spectra cannot be attributed to physicochemical effects.

**PAs by the Kinetic Method.** There are two PA scales currently accessible. One is the Lias et al.<sup>16</sup> collection, and the other is the more recent NIST compilation by Hunter and Lias<sup>17</sup> (used in Figure 2). The data given for alkanols are slightly different in the two collections and are not displaced by a common amount relating to the reestablishment of a single key alkanol PA. When peak height ratio data from the MI experiments were used, both scales produced plots that are satisfactory straight lines only if the reference PA for butanol is revised upward by 0.8 kcal mol<sup>-1</sup> (Figure 2). To emphasize the possible

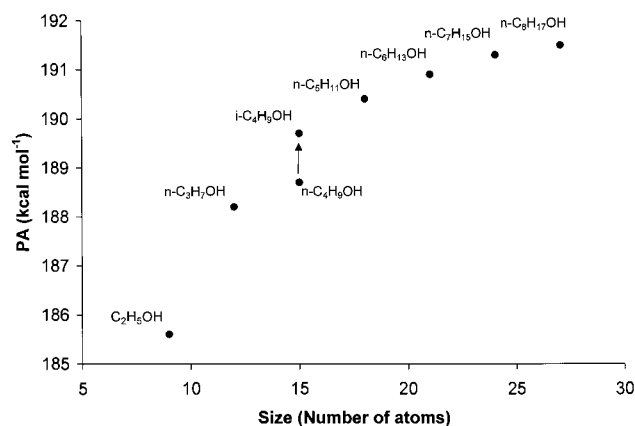


**Figure 3.** Plot of the PA of eight primary alkanols vs the number of atoms present in each. PA values are from ref 17 and the present work.

need for such a correction, it should be noted that the PA values for an *homologous* series change smoothly with the alkyl chain length, becoming asymptotic at high molecular weights.<sup>18,19</sup> This is illustrated in Figure 3; again the *n*-butanol value appears to need adjustment from 188.6 to 189.7 kcal mol<sup>-1</sup>. Finally, Figure 2 allows new PA values to be estimated, namely for *n*-pentanol (190 kcal mol<sup>-1</sup>) *n*-hexanol (191 kcal mol<sup>-1</sup>), *n*-heptanol (191 kcal mol<sup>-1</sup>), and *n*-octanol (191 kcal mol<sup>-1</sup>). These values are 2.7 kcal mol<sup>-1</sup> higher if the PAs from Lias et al.<sup>16</sup> are used in Figure 2. In view of the above discussion, it is difficult to confidently assign new PA values with a precision of more than three significant figures.

**Summary: The “Effective Temperature”.** It is now appropriate to ask whether the term “effective temperature” (as obtained from eq 3) relates to a thermodynamic property of these systems. On the basis of the results presented here, we believe that the plot of  $\ln([B_1H^+]/[B_2H^+])$  vs PA is no more than a semiempirical relationship, generally insensitive to changes of 10% or more in individual  $[B_1H^+]$  and  $[B_2H^+]$  values because the  $\ln$  function is used.<sup>20</sup> This is emphasized by Figure 2, in which the MI results give the best straight line, presumably because the peak ratio is large. Both the mixed MI and CID spectra and the isolated CID spectra results give smaller peak ratios and poorer correlations. This is not to detract from the usefulness of such relationships, which provide excellent routines for assessing new thermochemical data from known results on closely structurally related molecules.<sup>22</sup> We propose, therefore, that the use of a temperature-type term derived from such investigations be discontinued. Furthermore, the use of different target gases with the intention of observing different internal energy distributions also appears to be unjustified from the present results. We would further argue that, at least, *only* isolated CID mass spectra be recorded before any analysis of data is attempted.

**Acknowledgment.** The authors thank T. McMahon for advanced viewing of ref 6 and the reviewers of the manuscript for insightful comments. J.L.H. and P.M.M. thank the Natural Sciences and Engineering Research Council of Canada for financial support. P.M.M. also thanks the Chemistry Department, Faculty of Science and University of Ottawa, for a grant toward the purchase of the computer workstation.

## References and Notes

- (1) (a) Cooks, R. G.; Kruger, T. L. *J. Am. Chem. Soc.* **1977**, *99*, 1279–1281. (b) Cooks, R. G.; Patrick, J. S.; Kotah, T.; McLuckey, S. A. *Mass Spectrom. Rev.* **1994**, *13*, 287–339. (c) Harrison, A. G. *Mass Spectrom. Rev.* **1997**, *16*, 201–217.

- (2) (a) Kebarle, P. *Techniques for the Study of Ion–Molecule Reactions*; John Wiley and Sons: New York, 1988. (b) Schiff, H. I.; Bohme, D. K. *Int. J. Mass Spectrom. Ion Phys.* **1975**, *16*, 167–189. (c) Aue, D. H.; Webb, H. M.; Bowers, M. T. *J. Am. Chem. Soc.* **1976**, *98*, 311–317.
- (3) (a) Beauchamp, J. L.; Buttrill, S. E. *J. Chem. Phys.* **1968**, *48*, 1783–1789. (b) Long, J.; Munson, B. *J. Am. Chem. Soc.* **1973**, *95*, 2427–2432.
- (4) Baer, T.; Hase, W. L. *Unimolecular Reaction Dynamics*; Oxford University Press: New York, 1996.
- (5) Szulejko, J. E.; McMahon, T. B. *Int. J. Mass Spectrom. Ion Processes* **1991**, *109*, 279–294.
- (6) Norrman, K.; McMahon, T. B. *Int. J. Mass Spectrom. Ion Processes* **1998**, *176*, 87–97.
- (7) Holmes, J. L.; Cao, J. *Eur. Mass Spectrom.*, in press.
- (8) Holmes, J. L.; Mayer, P. M. *J. Phys. Chem.* **1995**, *99*, 1366–1370.
- (9) Bush, K. L.; Glish, G. L.; McLuckey, S. A. *Mass Spectrometry/Mass Spectrometry*; VCH Publishers: New York, 1988.
- (10) In an Arrhenius expression with  $E_a$  being ca. 30 kcal mol<sup>-1</sup>,<sup>11</sup> a frequency factor of  $10^{15}$  (appropriate for a loose transition state),<sup>12</sup> and a temperature of 420 K, only  $2.96 \times 10^{-4}\%$  of the ions will have sufficient energy to dissociate on the metastable time scale. In the present experiment, typically 1–10% of the adduct ions entering the third field-free region were metastable therein.
- (11) Larson, J. W.; McMahon, T. B. *J. Am. Chem. Soc.* **1982**, *104*, 6255–6261.
- (12) Holbrook, K. A.; Pilling, M. J.; Robertson, S. H. *Unimolecular Reactions*; Wiley: Chichester, 1996; Chapters 5 and 11.
- (13) Ab initio calculations were carried out with the GAUSSIAN 94<sup>14</sup> suite of programs, on an SGI Octane workstation, at the HF/6-31G(d) level of theory.
- (14) Frisch, M. J.; Trucks, G. W.; Schlegel, H. B.; Gill, P. M. W.; Johnson, B. G.; Robb, M. A.; Cheesman, J. R.; Keith, T.; Petersson, A.; Montgomery, A.; Ragavachari, K.; Al-Laham, M. A.; Zakrzewski, V. G.; Ortiz, J. V.; Foresman, J. B.; Cioslowski, J.; Stefanov, B. B.; Nanayakkara, A.; Challacombe, M.; Peng, C. Y.; Ayala, P. Y.; Chen, W.; Wong, M. W.; Andres, J. L.; Replogle, E. S.; Gomperts, R.; Martin, R. L.; Fox, D. J.; Binkley, J. S.; Defrees, D. J.; Baker, J.; Stewart, J. P.; Head-Gordon, M.; Gonzalez, C.; Pople, J. A. *GAUSSIAN 94*; Gaussian Inc.: Pittsburgh, PA, 1995.
- (15) Morgan, R. P.; Beynon, J. H.; Bateman, R. H.; Green, B. N. *Int. J. Mass Spectrom. Ion Phys.* **1978**, *28*, 171–191.
- (16) Lias, S. G.; Bartmess, J. E.; Liebman, J. F.; Holmes, J. L.; Levin, R. D.; Mallard, W. G. *J. Phys. Chem. Ref. Data* **1998**, *17* (Suppl. 1).
- (17) Hunter, E. P.; Lias, S. G. Proton Affinity Evaluation. In *NIST Chemistry WebBook, NIST Standard Reference Database Number 69*; Mallard, W. G., Linstrom, P. J., Eds.; National Institute of Standards and Technology: Gaithersburg, MD, 1998.
- (18) Gauld, J.; Holmes, J. L.; Radom, L. *Acta Chem. Scand.* **1997**, *51*, 641–645.
- (19) Anomalous behavior among *n*-alkyl species has been reported in solution studies where the acidities of *n*-alkanoic acids and *n*-alkylamines show an inversion from the ethyl to hexyl homologues. This does not appear to be the case here where only the butyl species appears anomalous. It is worth noting that the gas-phase acidities of the homologous alkanols show no such effect. Similar experiments in this laboratory with homologous amines and nitriles failed to show any discontinuities with increasing alkyl group size.
- (20) Using quantum RRR theory, Brauman and co-workers<sup>21</sup> have found that the relative rate constants for branching reactions can be related to the relative activation energies by a ln-linear relationship. They noted that the relationship was not universally applicable, however, nor is its validation of eq 1, which incorporates temperature as one of the principal variables.
- (21) Craig, S. L.; Zhong, M.; Choo, B.; Brauman, J. I. *J. Phys. Chem. A* **1997**, *101*, 19–24.
- (22) For examples, see: (a) Luo, Y.-R.; An, Y.; Holmes, J. L. *J. Mass Spectrom.* **1994**, *29*, 579. (b) Holmes, J. L.; Lossing, F. P. *Org. Mass Spectrom.* **1991**, *26*, 537–541.